J. Biochem. 2010;147(4):565–579 doi:10.1093/jb/mvp203

JB THE JOURNAL OF BIOCHEMISTRY

Identification and characterization of nCLP2, a novel C1q family protein expressed in the central nervous system

Received October 26, 2009; accepted November 30, 2009; published online December 8, 2009

Chisei Shimono[1,2], Ri-ichiroh Manabe[1,2], Tomiko Yamada[2], Shiro Fukuda[3], Jun Kawai[3], Yutaka Furutani[2], Ko Tsutsui[1,2], Kazuhiro Ikenaka[4], Yoshihide Hayashizaki[3] and Kiyotoshi Sekiguchi[1,2,*]

[1]Institute for Protein Research, Osaka University, Suita, Osaka 565-0871; [2]Sekiguchi Biomatrix Signaling Project, Japan Science and Technology Agency, c/o Aichi Medical University, Nagakute, Aichi 480-1195; [3]RIKEN Omics Science Center, RIKEN Yokohama Institute, Yokohama, Kanagawa, 230-0045; and [4]National Institute for Physiological Sciences, Okazaki, Aichi 444-8787, Japan

*Kiyotoshi Sekiguchi, Institute for Protein Research, Osaka University, 3-2 Yamadaoka, Suita, Osaka 565-0871, Japan, Tel: +81 6 6879 8617, Fax: +81 6 6879 8619, E-mail: sekiguch@protein.osaka-u.ac.jp

The C1q family is characterized by the C-terminally conserved globular C1q (gC1q) domain. Although more than 30 C1q family proteins have been identified in mammals, many of them remain ill-defined with respect to their molecular and biological properties. Here, we report on a novel C1q family protein specifically expressed in the central nervous system (CNS), which we designated neural C1q-like protein (nCLP) 2. nCLP2 was secreted as disulphide-bonded multimers comprising trimeric units. The multimers were stabilized by interchain disulphide bonds involving the cysteine residues in the N-terminal variable region and the C-terminal gC1q domain. The expression of nCLP2 was restricted to several brain regions and retina, including regions associated with memory formation (*i.e.* hippocampus, entorhinal cortex, anterodorsal thalamic nucleus). Immunoelectron microscopy revealed that nCLP2 was localized in the mossy fibre axons of hippocampal granule cells and their synaptic boutons and clefts, implying that nCLP2 was anterogradely transported in mossy fibres and secreted from the presynaptic termini. These results suggest that nCLP2 plays roles in synaptic function and maintenance in the CNS.

Keywords: Brain/complement/neuron/secretion/self-assembly.

Abbreviations: BDNF, brain-derived neurotrophic factor; BS^3, *bis*(sulphosuccinimidyl) suberate; BSA, bovine serum albumin; Cbln, cerebellin; CNS, central nervous system; DIG, digoxigenin; gC1q, globular C1q; HMW, high molecular weight; ISH, *in situ* hybridization; MALDI-TOF-MS, matrix-assisted laser desorption ionization time-of-flight mass spectrometry; nCLP, neural C1q-like protein; ORF, open reading frame.

The C1q family is a group of proteins characterized by a C-terminally conserved globular C1q (gC1q) domain, which was first identified in the q subcomponent of the complement C1 complex (*1*). Currently, more than 30 genes encoding C1q family proteins have been found in mammals (*2*). Most C1q family proteins are secreted proteins with a domain structure comprising an N-terminal secretion signal peptide, collagen triple helical repeats and a C-terminal gC1q domain (*2*, *3*). The gC1q domain has a 10-strand jelly-roll folding topology that is similar to the fold of the tumour necrosis factor family proteins, suggesting an evolutionary link between these two families (*4*), both implicated in immunity and energy homeostasis (*3*). The gC1q domain forms a trimer of β-sandwich protomers. The trimeric units of C1q family proteins often associate via disulphide bonds to yield hexamers, which in turn assemble into multimers with a bouquet-like configuration (*3*, *5*). Multimer formation is crucial for exerting the biological functions of particular C1q family proteins (*6*, *7*).

The C1q family proteins have been shown to play roles in diverse aspects of physiological and pathological processes (*1*). The complement C1q protein acts as the target recognition protein of the classical complement pathway and is a major link between innate and acquired immunity (*1*,*3*). The deficiency of this protein is a likely cause of systemic lupus erythematosus, resulting in an impaired clearance of apoptotic cells (*8*). Adiponectin, a serum protein abundantly expressed in adipose tissue, has been extensively studied due to its anti-diabetic, anti-atherogenic and anti-inflammatory activities (*9*). Decreased serum levels of adiponectin have been associated with type 2 diabetes (*10*). Cartducin, a paralog of adiponectin, is induced during chondrogenic differentiation and stimulates the proliferation of mesenchymal chondroprogenitor cells in skeletal development (*11*). Given their nature as secreted proteins, some C1q family proteins have been localized at extracellular matrices including elastic fibres and subendothelial and cartilaginous matrices (*3*). For example, EMILIN-1 is associated with elastic fibres in blood and lymphatic vessels and deficiencies of this protein in mouse models results in increased blood pressure due to increased transforming growth factor-β signaling (*12*). Collagen X is a short chain collagen containing the gC1q domain, mutations in which have been closely associated with Schmid metaphyseal chondrodysplasia (*7*), an autosomal dominant skeletal disorder characterized by growth plate abnormalities, short stature and a waddling walk.

Some C1q family proteins are selectively expressed in the central nervous system (CNS). Cerebellin (Cbln)

1, a C1q family protein predominantly expressed in cerebellar granule cells, is implicated in the formation and stabilization of synaptic contacts and the control of functional synaptic plasticity by regulating the post-synaptic endocytosis pathway (*13*). Other Cbln members, Cblns2–4, are expressed in various regions of developing and mature brains (*14*), likely exerting their functions similar to those of Cbln1 (*15*). Besides Cbln members, a C1q family protein termed 'C1q-related factor' is highly expressed in the brain regions involved in motor function, including Purkinje cells, the accessory olivary nucleus, the pons and the red nucleus (*16*). C1q-like 3, another C1q family protein closely related to the C1q-related factor, has been compiled in the public database as a protein predominantly expressed in glial cells (LOC684921; http://www.ncbi.nlm.nih.gov); however, the function of C1q-like 3 remains unexplored. Some other C1q family proteins have also been shown to act on brain regions. Thus, adiponectin enhances the activity of AMP-activated protein kinase in the arcuate hypothalamus and thereby stimulates food intake (*17*). Complement C1q protein is transiently expressed in postnatal neurons and mediates synapse remodelling in the developing brain (*18*, *19*). However, it remains to be explored whether other C1q family proteins are also expressed in the CNS and regulate brain functions.

In this study, we report a hitherto functionally unknown C1q family protein, which we identified in our transcriptome-wide systematic screening for novel secreted proteins expressed at high levels in the CNS. This protein, which we designated 'neural C1q-like protein (nCLP) 2′, is highly expressed in the hippocampus and localized in the synaptic termini and synaptic clefts at the stratum lucidum of the hippocampus. We provide evidence that nCLP2 is a secreted protein forming high molecular weight (HMW) multimers in a trimer assembly manner, as has been demonstrated for adiponectin and other C1q family proteins.

Materials and Methods

Animals

ICR mice and Sprague Dawley rats were purchased from Japan SLC (Hamamatsu, Japan). The animals and procedures used in this study were in accordance with the guidelines approved by Animal Care and Use Committees of Aichi Medical University and Osaka University.

Transcriptome-based systematic screening for extracellular proteins predominantly expressed in the CNS

Complementary DNA clones encoding novel extracellular proteins were computationally screened from the RIKEN mouse full-length enriched cDNA collections as described previously (*20*). Briefly, cDNAs encoding putative secreted proteins were selected from >75,000 entries of the RIKEN's mouse cDNA collections (*21*), based on the presence of a secretion signal sequence at the N-terminus and the absence of any other transmembrane anchor sequences in an entire open reading frame (ORF), as judged by PSORT II (*22*) and SOSUI (*23*), respectively. Functionally known proteins were eliminated by homology searches using FASTA (*24*). cDNA clones predominantly expressed in CNS tissues were then selected by *in silico* differential display using EST datasets compiled in the RIKEN FANTOM databases (http://fantom3.gsc.riken.jp/) and UniGene databases (http://www.ncbi.nlm.nih.gov). For details, see the 'Results' section.

cDNA cloning, plasmid construction, and recombinant protein expression and purification

Standard PCR techniques were used in cDNA cloning and mutagenesis. The oligonucleotide primers used in this study are listed in Supplementary Table SI. cDNAs encoding the entire ORFs of nCLP1, nCLP3 and nCLP4 were obtained by RT-PCR using the RNA extracted from the mouse brain (Clontech, Mountain View, CA, USA) as templates. The nucleotide sequences of the PCR products were verified by DNA sequencing from both directions. The cDNAs were subcloned into pFLAG-CMV-5a (Sigma, St. Louis, MO, USA) at EcoRI/KpnI (for nCLP1, 2, 3) or EcoRI/BamHI (for nCLP4) sites. The cysteine-substituted mutants of nCLP2 and adiponectin were generated by standard PCR-based mutagenesis using primer pairs listed in Supplementary Table S1. Recombinant proteins were expressed and purified as described previously (*25*). Briefly, Freestyle™ 293F cells (Invitrogen, Carlsbad, CA, USA) were transfected with pFLAG-CMV-5a constructs encoding full-length proteins with a C-terminal FLAG tag and cultured in Freestyle™ 293F medium (Invitrogen) containing 50 μg/ml ascorbic acid for 2 days. The recombinant proteins were purified from the conditioned media by immunoaffinity chromatography using an anti-FLAG M2 monoclonal antibody (Sigma).

RT–PCR

The transcripts of nCLPs were reverse-transcribed from total RNA extracted from various mouse tissues (Clontech) and amplified by PCR using the pairs of forward and reverse primers (see Supplementary Table SI) and LA Taq DNA polymerase (Takara Bio Inc., Otsu, Japan) with the following cycling conditions: 94°C for 30 s, 58°C (nCLPs 1–3) or 56°C (nCLP4) for 30 s and 72°C for 2 min. The PCR cycle was repeated 30 times for nCLP1–3 and 35 times for nCLP4. The expression of mouse β-actin transcripts was monitored as a control under the same PCR conditions.

Antibodies

Two anti-nCLP2 antibodies, anti-nCLP2-V and anti-nCLP2-S, were raised in rabbits using synthetic peptides GPSTAALEVMQDLSA NPP (amino acids 53–70) and GGDTEGEVTSALSAAFSG (amino acids 139–156) as immunogens after conjugation to keyhole limpet hemocyanin. Antibodies were purified by affinity chromatography using antigenic peptides immobilized on Thiopropyl Sepharose™ 6B (GE Healthcare, Piscataway, NJ, USA). Bound antibodies were eluted with 100 mM glycine, pH 2.5, neutralized with Tris-HCl (pH 8.5), and then dialysed against phosphate buffered saline (PBS). Specificities of affinity-purified antibodies were verified by immunoblot analyses of conditioned media and cell extracts of 293F cells transfected with individual nCLP cDNAs.

SDS–PAGE and immunoblotting

SDS–PAGE was carried out according to Laemmli (*26*). Samples were dissolved in Laemmli's sample treatment buffer and heated to 95°C for 10 min prior to loading on gels. Dithiothreitol was added to the sample treatment buffer at a final concentration of 100 mM when samples were reduced. For immunoblotting, proteins separated on 10–20% gradient gels were transferred to Hybond-ECL membranes (GE Healthcare). The membranes were then blocked with 5% (w/v) skim milk in TBS containing 0.05% Tween 20 (TBS-T) and incubated with anti-FLAG M2 antibody (1:1,000 dilution) or the affinity-purified anti-nCLP2 antibody (5 μg/ml) in TBS-T containing 5% skim milk for 1 h at room temperature. After washing with TBS-T, the membranes were incubated with horseradish peroxidase-conjugated anti-mouse immunoglobulin G $F(ab')_2$ fragments or horseradish peroxidase-conjugated anti-rabbit immunoglobulin G $F(ab')_2$ fragments (1:4,000 dilution) for 30 min at room temperature and then washed thoroughly. Bound antibodies were visualized using ECL Western blotting detection reagents (GE Healthcare).

Chemical crosslinking

Recombinant proteins dissolved in PBS at 20 μg/ml were mixed with an equal volume of PBS containing bis(sulphosuccinimidyl) suberate (BS^3) (Thermo Scientific, Rockland, IL, USA) at increasing concentrations (0.002, 0.02, 0.2, 2, and 20 mg/ml), and incubated for 30 min at room temperature. Reactions were quenched by incubation with 50 mM Tris–HCl (pH 8.0) for 15 min at room temperature.

Crosslinked proteins were analysed by SDS–PAGE and the following immunoblotting.

In situ hybridization

nCLP2 transcripts were detected by *in situ* hybridization *(ISH)* using digoxigenin (DIG)-labelled antisense riboprobes. The cDNA templates for antisense probes were amplified by PCR using different pairs of primers (nCLP2-5′probeF/R and nCLP2-3′probeF/R; see Supplementary Table SI) and subcloned into pCR-Blunt II TOPO with a Zero Blunt TOPO PCR Cloning Kit (Invitrogen). DIG-labelled single-stranded riboprobes were prepared by transcription of linearized plasmids using T7 or Sp6 RNA polymerase and a DIG RNA labelling kit (Roche, Basel, Switzerland). ISH staining was performed as reported previously (*27*). Briefly, 10 μm sections of adult mouse brains were fixed with 4% formaldehyde in PBS, permeabilized with 10 μg/ml proteinase K in 50 mM Tris–HCl (pH 7.5) and 5 mM EDTA, and acetylated in 0.1 M triethanolamine buffer containing 0.2% acetic anhydride. The sections were then hybridized with 0.5 μg/ml DIG-labelled probes in hybridization buffer containing 50% formamide, 20 mM Tris–HCl (pH 7.5), 600 mM NaCl, 1 mM EDTA, 10% dextran sulphate, 200 μg/ml yeast tRNA, 1 × Denhardt's solution and 0.25% SDS at 65°C overnight. The sections were washed three times with 1 × SSC containing 50% formamide at 65°C, followed by 0.1 M maleic buffer (pH 7.5) containing 0.1% Tween 20 and 0.15 M NaCl. The DIG-labelled probes were visualized by overnight incubation with an anti-DIG antibody conjugated to alkaline phosphatase (1:2,000 dilution), followed by colour development with nitro blue tetrazolium chloride (NBT)/BCIP (5-bromo-4-chloro-3-indolyl phosphate, toluidine salt) solution (Roche). Both probes gave similar results, verifying the specificity of our ISH probes.

Immunohistochemical staining

Unfixed tissue specimens obtained from 9-week-old ICR mice were embedded in an OCT compound (Sakura Finetechnical, Tokyo, Japan) and were subsequently frozen. Cryosections (10 μm thick) were blocked with 5% (w/v) bovine serum albumin (BSA) in PBS for 30 min at room temperature and then incubated with affinity-purified antibodies against nCLP2 (1 μg/ml) overnight at 4°C, followed by incubation with AlexaFluor 488-conjugated anti-rabbit IgG (1:200 dilution; Molecular Probes, Eugene, OR, USA) for 1 h. The sections were counterstained with Hoechst 33342 (1:100,000 dilution). The specificity of the antibodies used was verified by their almost identical staining patterns and by the absorption of their immunoreactivities with antigenic peptides.

Immunoelectron microscopy

Deeply anesthetized 9-week-old ICR mice were transcardially perfused with 100 ml of PBS, followed by 100 ml of 4% paraformaldehyde in PBS, and dissected. Fixed brains were sliced as horizontal vibratome sections (50 μm thick) in ice-chilled PBS. The sections were blocked with 5% BSA and incubated with the anti-nCLP2 antibody (5 μg/ml) overnight at 4°C. After washing with PBS, the sections were incubated with a secondary goat anti-rabbit IgG conjugated to 1 nm gold particles (1:50 dilution; British Biocell International, Cardiff, UK) in PBS containing 5% BSA. Signals labelled with gold particles were enhanced with a silver intensification kit (British Biocell International). The immunogold-labelled sections were postfixed with 1% osmium tetroxide in 0.1 M phosphate buffer (pH 7.4) for 1 h at 4°C and dehydrated in a stepwise manner with 80, 90, 99, 100% ethanol and propylene oxide. Sections were mounted with Epon 812 on siliconized glass slides. Sections containing stratum lucidum of the hippocampus were cut out under a light microscopic observation and ultrathin-sliced with an ultramicrotome (LKB, Bromma, Sweden) at a thickness of 80 nm. Ultrathin sections were stained with lead citrate and examined using a JEM-2000EX transmission electron microscope (JEOL Ltd, Tokyo, Japan).

Gel filtration chromatography

Purified proteins (50 μg in 100 μl PBS) were loaded onto a Cosmosil 5Diol-II column (300 × 7.5 mm, 11 ml void volume; Nacalai Tesque, Kyoto, Japan) which had been equilibrated with 0.02 M phosphate buffer (pH 7.0) containing 0.1 M NaCl. Proteins were eluted with the same buffer at a flow rate of 1 ml/min and monitored by absorbance at 280 nm. The column was calibrated using the molecular weight marker proteins: bovine carbonic anhydrase (MW, 29,000), bovine serum albumin (MW, 66,000), yeast alcohol dehydrogenase (MW, 150,000), potato β-amylase (MW, 200,000), horse apoferritin (MW, 443,000) and bovine thyroglobulin (MW, 669,000). All marker proteins were purchased from Sigma.

Matrix-assisted laser desorption ionization time-of-flight mass spectrometry (MALDI-TOF-MS)

Purified recombinant nCLP2 was treated with porcine trypsin (20 μg/ml; Wako, Osaka) at 37°C overnight and subjected to reversed-phase high performance liquid chromatography on a Develosil 300C8-HG column (150 × 4 mm; Nomura Inc., Aichi, Japan). After washing with 80% acetonitrile containing 0.1% (v/v) trifluoroacetic acid, peptides were eluted with a 60 min linear gradient of 10–80% acetonitrile at a flow rate of 500 μl/min and collected in 500 μl fractions. An aliquot (2 μl) of each fraction was mixed with an equal volume of matrix (10 mg/ml α-cyano-4-hydroxycinnamic acid dissolved in 50% acetonitrile with 0.1% trifluoroacetic acid), spotted onto a sample plate and allowed to dry. The samples were then analysed using Autoflex III MALDI-TOF-MS (Bruker Daltonics Inc., Bremen, Germany). Reflectron mass spectrometric analyses were performed on Autoflex workstation (Bruker Daltonics Inc.) using a pulsed laser beam (nitrogen laser, $\lambda = 337$ nm). All ion spectra were recorded in the positive mode with an accelerating voltage of 20.0 kV. The spectrometer was externally calibrated using a Cal Mix 2 standard mixture (PerSeptive Biosystems Inc., Framingham, MA, USA).

Results

Identification of novel C1q-like proteins expressed in the CNS

RIKEN mouse full-length enriched cDNA collections comprising more than 75,000 cDNAs (*21*) were computationally screened for those encoding novel secreted proteins as described previously (*20*). The selected cDNAs were subjected to *in silico* differential display using ESTs compiled in UniGene and RIKEN FANTOM databases (*21*) to identify proteins selectively expressed in the CNS. In the computational differential display, we employed an 'EST score', a ratio of the number of ESTs derived from CNS tissues to those from all tissues including the CNS, as a measure of selective CNS expression for a given cDNA. In a pilot study, we determined the EST scores of 36 full-length cDNAs that had been selected in the initial computational screening for those encoding novel secreted proteins. Determination of their expression levels in various tissues by RT-PCR revealed that nine of these genes were highly expressed in the CNS. Eight out of the nine cDNAs gave EST scores of >0.6, prompting us to employ >0.6 as a threshold in selecting candidate cDNAs encoding proteins highly expressed in the CNS. We determined the EST scores of 71 cDNA clones obtained from computational screening for those encoding novel secreted proteins and 23 cDNAs were found to have an EST score of >0.6. Twelve of the genes were confirmed by RT-PCR for their significant expression in CNS tissues (*i.e.* brain, spinal cord and eye); however, some of the genes were also expressed in other organs (Supplementary Fig. S1).

To further confirm their CNS expression at the protein level, we produced rabbit antibodies against the candidate proteins and examined immunohistochemically their expression in CNS tissues. Seven candidate proteins were specifically localized in the nervous system, of which the protein encoded by the clone #G630075L11 gave highly restricted signals at the

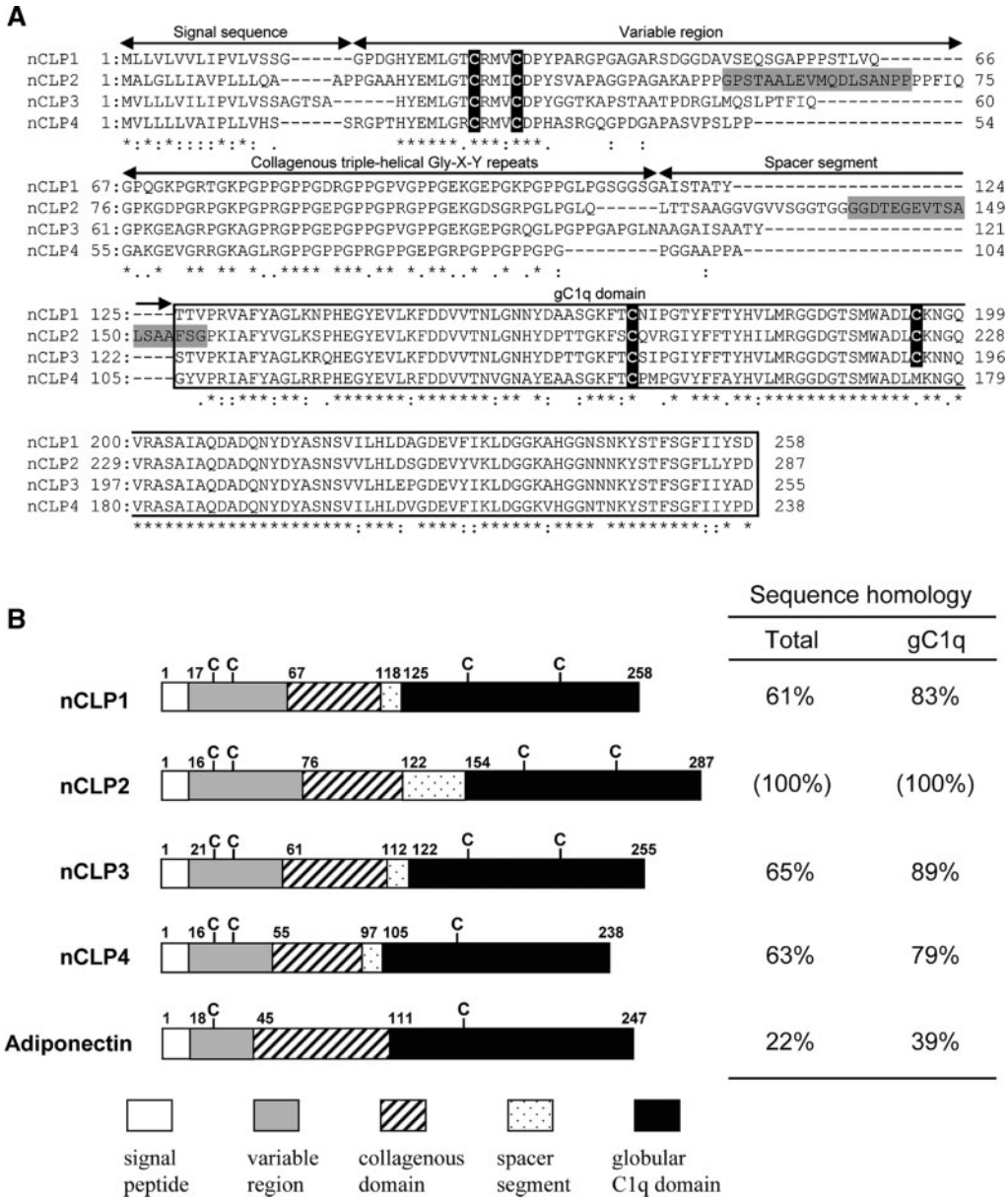

Fig. 1 Primary structure of mouse nCLPs. (A) Sequence alignment of the four nCLPs. Predicted signal sequences, variable regions, collagenous triple-helical Gly-X-Y repeats and spacer segments are indicated above the sequences. The gC1q domains are boxed. Cysteine residues are highlighted in black with white letters. Identical, conserved and semi-conserved residues between the nCLPs are marked with asterisk, colon and dot, respectively. The sequences of immunogenic peptides for producing anti-nCLP2 antibodies (Gly^{53}–Pro^{70} for anti-nCLP2-V; Gly^{139}–Gly^{156} for anti-nCLP2-S) are colored in gray. (B) Domain structures of nCLPs and adiponectin. nCLPs and adiponectin share the same modular organization, consisting of a signal peptide, a variable region, a collagenous domain, a spacer segment and a gC1q domain. The numbers above the schemes indicate the positions of the first amino acid residues of individual regions. The locations of cysteine residues (C) are shown above the schemes. Sequence homologies between the four nCLPs and adiponectin are shown on the right.

CA3 region of the hippocampus (see below). The cDNA clone encodes a 287 amino acid polypeptide comprising an N-terminal signal sequence, a collagenous domain and a C-terminal gC1q domain (Fig. 1A) and has been registered as 'complement component 1, q subcomponent-like 2' in the public domain databases (*e.g.* http://www.ncbi.nlm.nih.gov). Homology searches of genomic and EST databases identified three other cDNAs that encode proteins with >60% overall homologies; *i.e.* 'complement component 1, q subcomponent-like 1' [also called C1q-related factor (*16*)], 'C1q-like 3', and 'complement component 1, q subcomponent-like 4'. These proteins including the protein encoded by the clone #G630075L11 were 'C1q-like proteins' characterized by the C-terminal gC1q domain preceded by a collagenous domain. Since the genes encoding these C1q-like proteins are predominantly expressed in the nervous tissues (see below), we coined the name 'neural C1q-like proteins (nCLPs)' for these four proteins and designated the protein encoded by the clone #G630075L11 as nCLP2. The other three proteins were designated as nCLP1, nCLP3 and nCLP4. The phylogenic analysis showed that the four nCLPs comprised a distinct

subgroup within a total of 30 mouse C1q family proteins (Supplementary Fig. S2), exhibiting a significantly high homology in the gC1q domain (Fig. 1B).

nCLP2 contains a 60 amino acid segment N-terminal to the collagenous domain, where two cysteine residues are located (Fig. 1A). Since the length of this N-terminal segment varies among nCLPs and other C1q family proteins, this segment is hereafter referred to as the 'N-terminal variable region'. nCLP2 contains four cysteine residues, two in the N-terminal variable region (Cys-29 and Cys-33) and two in the C-terminal gC1q domain (Cys-197 and Cys-224). These cysteine residues are conserved among the nCLPs except that nCLP4 lacks the cysteine residue equivalent to Cys-224 in nCLP2. The cysteine residue conserved in the gC1q domain of all four nCLPs, *e.g.* Cys-197 in nCLP2, is also found in many other C1q family proteins including the complement C1q protein and adiponectin.

nCLP2 is a secreted protein

To confirm that nCLP2 and the other nCLPs are secreted proteins, four nCLPs were expressed in 293F cells with a FLAG epitope tag at their C-termini. The culture supernatants were collected and subjected to immunoblot analyses using an anti-FLAG antibody. Under reducing conditions, nCLP2 was detected at the 28–32 kDa region as triplet bands (Fig. 2), consistent with its predicted molecular mass (30 kDa). Other nCLPs were also detected at positions equivalent to their predicted molecular masses (nCLP1, 27 kDa; nCLP3, 26 kDa; nCLP4, 25 kDa). Similar results were also obtained when nCLP2 was expressed in COS and 293T cells (data not shown). Under non-reducing conditions, nCLP2 gave bands at the 60, 120 and 180 kDa regions, each corresponding to the dimer, tetramer and hexamer, respectively. No bands were detected at the monomer position under non-reducing conditions. Other nCLPs also gave bands at dimer and tetramer positions but not at the monomer position. Putative hexamer bands were barely detectable for other nCLPs. These results indicate that all nCLPs are secreted as disulphide-bonded oligomers/multimers, as has been demonstrated for other C1q family proteins (*28*).

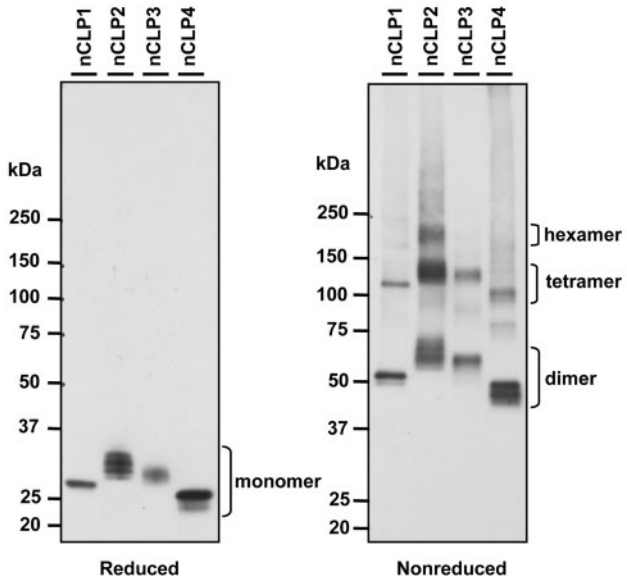

Fig. 2 Immunoblot analysis of recombinant nCLPs secreted by 293F cells. Conditioned media of 293F cells transfected with C-terminally FLAG-tagged nCLPs were subjected to SDS–PAGE using 5–20% gradient gels under reducing and non-reducing conditions. Recombinant proteins were detected by immunoblotting using an anti-FLAG antibody. Bands corresponding to monomer, dimer, tetramer and hexamer of nCLPs are indicated on the right. Under non-reducing conditions, bands representing nCLP2 were observed at 60,120 and 180 kDa, each corresponding to the dimer, tetramer and hexamer species, respectively. No bands at the monomer position were detected under non-reducing conditions.

The apparent heterogeneity of the secreted nCLP2 is likely to be due to the differential degree of posttranslational modifications such as glycosylation of asparagine, serine/threonine and hydroxylysine residues and/or hydroxylation of proline and lysine residues. Hydroxylation of proline and lysine residues occurring in the collagenous domain has been shown to be crucial for stabilizing the oligomeric complexes of adiponectin (*29*, *30*). To examine whether the collagenous domain of nCLP2 was hydroxylated, purified recombinant nCLP2 was trypsinized and subjected to matrix-assisted laser desorption ionization time-of-flight mass spectrometry. The mass spectra indicated that a peptide encompassing Gly^{91}–Pro^{102} was differentially hydroxylated at three proline residues located at Y-positions (Supplementary Fig. S3). Such heterogeneity in proline hydroxylation has been shown to give rise to microheterogeneity in banding patterns of collagenous proteins upon SDS–PAGE (*30*, *31*).

nCLP2 is selectively expressed in CNS tissues

To explore the CNS expression of nCLP2 and the other nCLPs, the tissue expression profiles of nCLP transcripts were investigated by RT-PCR using total RNAs extracted from a panel of 22 mouse adult organs including brain, spinal cord, eye and embryonic brains. Consistent with the results obtained by computational differential display and preliminary RT-PCR screening, nCLP2 transcripts were only detected in the CNS organs (*i.e.* brain, spinal cord and eye), but not in other organs except for the placenta (Fig. 3). In embryonic brains, the nCLP2 transcripts were not detected at embryonic day 12, but became detectable at embryonic day 14 and throughout the following embryonic stages.

Like nCLP2, nCLP1 and nCLP3 were almost exclusively expressed in the CNS tissues, except that nCLP1 was expressed in the uterus and nCLP3 in the kidney (Fig. 3). In contrast, nCLP4 transcripts were detected not only in the CNS but also in other organs. Furthermore, the expression levels of nCLP4 in the brain and other CNS organs were less pronounced than those in non-CNS organs.

In situ detection of nCLP2 transcripts in the adult mouse brain

To determine the loci where nCLP2 is expressed in the CNS, nCLP2 transcripts was localized in the adult brain by *in situ* hybridization. Signals for nCLP2

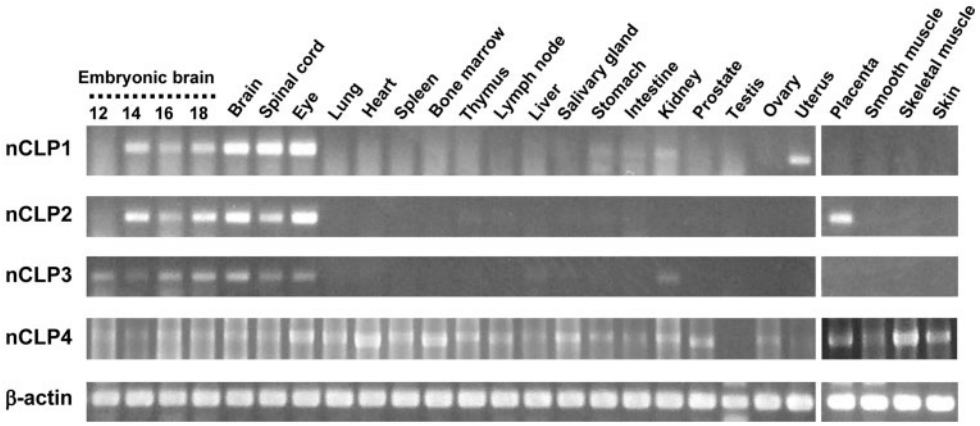

Fig. 3 Expression of nCLP transcripts in embryonic brain and adult tissues. Expression of nCLP transcripts were analysed by RT-PCR using total RNA derived from mouse brains of embryonic day 12, 14, 16 and 18 embryos and from a variety of adult tissues. Transcripts for nCLPs 1–3 and β-actin were amplified for 30 PCR cycles and those for nCLP4 were amplified for 35 cycles. In adult tissues, nCLPs 1–3 were predominantly expressed in the CNS, *i.e.* brain, spinal cord and eye, whereas nCLP4 transcripts were ubiquitously detected in most organs. nCLPs were also expressed in embryonic brains.

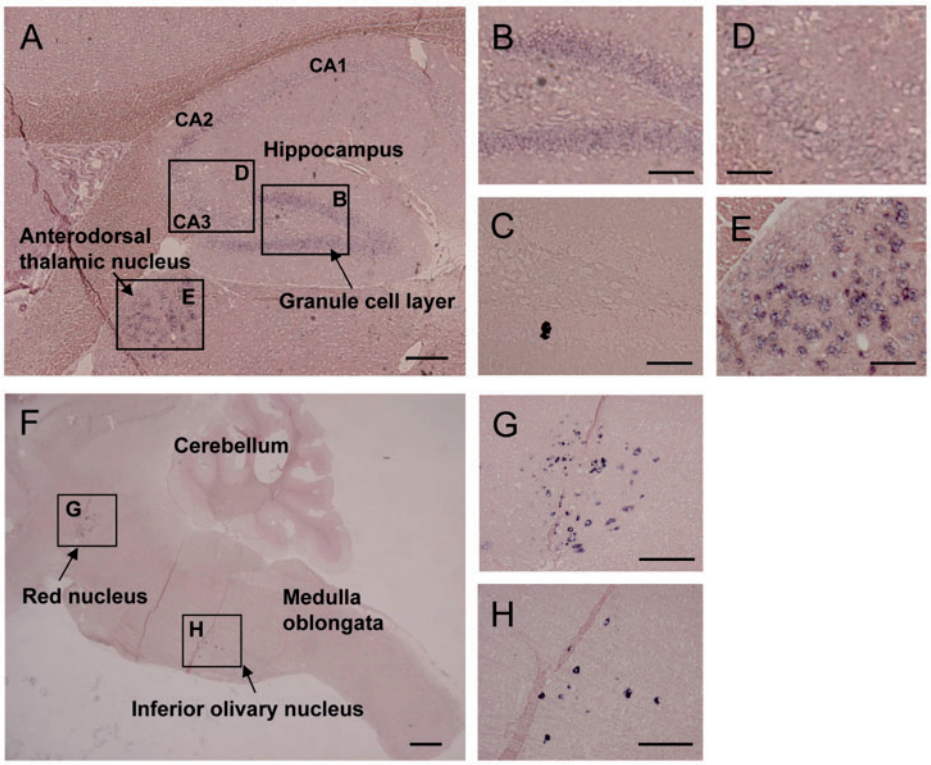

Fig. 4 ISH of nCLP2 transcripts in adult brain. Antisense riboprobes labelled with digoxigenin were hybridized to sagittal sections of a 9-week-old mouse brain. nCLP2 transcripts were expressed in the hippocampal granule cell layer (A and B). (C) shows a negative control image with a sense riboprobe for the hippocampal granule cell layer. There were no signals detected in the CA3 pyramidal cell layer (A and D). nCLP2 transcripts were also expressed in the anterodorsal thalamic nucleus (A, E), the red nucleus (F and G) and the inferior olivary nucleus (F and H). (B, D, E, G and H) show high-power views of boxed areas in panels A and F. The bar represents 200 μm in (A, G and H), 100 μm in (B–E) and 500 μm in (F).

transcripts were detected in the hippocampus and some nerve nuclei in the brain (Fig. 4). In the hippocampus, nCLP2 transcripts were highly expressed in the granule cells of dentate gyrus and, to a lesser extent, in the pyramidal cells of the CA2 region, whereas no transcripts were detected in other regions including the CA3 regions of the hippocampus (Fig. 4A–D). In other regions of the brain, nCLP2 transcripts were detected in the anterodorsal thalamic nucleus, red nucleus and inferior olivary nucleus (Fig. 4A, E, F–H).

Immunohistochemical localization of nCLP2 in the adult brain and eye

To further investigate the expression of nCLP2 in CNS tissues, we produced two separate rabbit antibodies,

one directed to the N-terminal variable region (anti-nCLP2-V) and the other directed to the spacer region between the collagenous domain and the gC1q domain (anti-nCLP2-S). The sequences of the antigenic peptides are indicated in Fig. 1A. These antibodies were affinity-purified on agarose beads conjugated with the antigenic peptides and showed no cross-reactivities against other nCLPs on immunoblotting (Supplementary Fig. S4). Immunohistochemical staining of adult brains with anti-nCLP2-S showed that nCLP2 was predominantly localized in the stratum lucidum of the hippocampus, where the mossy fibres, *i.e.* the nerve axons projecting from granule neurons of the dentate gyrus, form synapses with thorny excrescences of dendrites of CA3 pyramidal cells (Fig. 5A and B). The localization of the nCLP2 protein in the stratum lucidum was verified by immunohistochemical staining with another antibody, anti-nCLP2-V (data not shown). Given that nCLP2 transcripts were highly expressed in the granule cells of the dentate gyrus (see Fig. 4A and B), these results indicate that nCLP2 is produced in the granule cells and transported through mossy fibres towards the pyramidal cells in the CA3 region.

The immunohistochemical signals for nCLP2 were also detected in the anterodorsal thalamic nucleus, red nucleus and inferior olivary nucleus (Fig. 5C–F), where nCLP2 transcripts were detected by *in situ* hybridization. Furthermore, signals were detected at neurons in the third layer of the entorhinal cortex (Fig. 5G).

We also examine the localization of the nCLP2 protein in the eye. The signals for nCLP2 were detected only in retina, specifically at inner and outer plexiform layers and amacrine cells in the inner nuclear layer (Fig. 5H). Since inner and outer plexiform layers in retina are rich in synapses, as is the case with the stratum lucidum in the hippocampus, these results together imply that nCLP2 may be involved in formation, maintenance and/or functions of synapses in these regions.

Immunoelectron microscopic localization of nCLP2 in the hippocampus

The characteristic expression of nCLP2 in the hippocampus prompted us to extend the microscopic localization of nCLP2 to a greater depth. We examined the localization of nCLP2 in the stratum lucidum of the hippocampus by immunoelectron microscopy and found that nCLP2 was localized in mossy fibres and synaptic boutons, huge synaptic termini of granule cell axons (Fig. 6A and B). nCLP2 signals were also detected in the synaptic clefts between synaptic boutons and dendritic spines of CA3 pyramidal cells (Fig. 6B and C), indicating that nCLP2 expressed by granule cells in the dentate gyrus was transported towards synaptic termini through mossy fibres and finally secreted from the synaptic termini to the synaptic clefts.

Molecular organization of nCLP2 multimers

Given that nCLP2 was secreted from synaptic termini of mossy fibres and that recombinant nCLP2 was secreted from transfected 293F cells as disulphide-bonded oligomers, we sought to explore the mechanism of how nCLP2 forms disulphide-bonded oligomers, focusing on the cysteine residues involved in oligomer formation. Cysteine residues in the N-terminal variable region have been shown to be responsible for disulphide-bonded oligomer formation of C1q family proteins (*6*, *28*, *32*). As such, nCLP2 mutants were produced in which either or both of the cysteine residues in the N-terminal variable region (*i.e.* Cys-29 and Cys-33) were substituted with serine residues. SDS–PAGE under non-reducing conditions showed that mutant proteins with single substitution of either Cys-29 or Cys-33 gave multiple bands migrating at dimer and oligomer positions but not at the monomer position (Fig. 7). In contrast, the mutant nCLP2 with double substitution of both Cys-29 and Cys-33 gave a significant band migrating at the monomer position, indicating that both cysteine residues in the N-terminal variable region were involved in disulphide-bonded dimer/oligomer formation. However, a fraction of the double substitution mutant still remained as disulphide-bonded dimer and tetramer, raising the possibility that cysteine residues in the C-terminal gC1q domain were also involved in disulphide-bonded dimer/oligomer formation. To address the possibility, we produced a mutant nCLP2 in which all four cysteine residues were substituted with serine residues. The resulting mutant protein, designated nCLP2-all-CS, migrated almost exclusively at the monomer position, supporting this possibility.

To further explore the oligomeric states of nCLP2 proteins, recombinant nCLP2 was size-fractionated by gel filtration chromatography. Adiponectin, another C1q family protein with molecular size and domain structure close to those of nCLP2 (Fig. 1B), was also recombinantly produced and subjected to size fractionation as a control. The oligomeric states of adiponectin have been extensively studied by gel filtration chromatography (*6*, *28*, *33*). Adiponectin was resolved into four peaks, each corresponding to two forms of high molecular weight (HMW) multimers, hexamers and trimers (Fig. 8A), whereas nCLP2 was resolved into two molecular species, a major one with apparent molecular mass of >700 kDa and a minor one with that of 600 kDa, both of which were considered to represent HMW multimers based on their elution positions (Fig. 8B). These results indicated that recombinant nCLP2 secreted from transfected 293F cells was prone to form HMW multimers rather than hexamers and trimers.

The cysteine residue in the N-terminal variable region of adiponectin has been shown to be crucial for HMW multimer formation (*6*, *28*). To examine whether two cysteine residues in the N-terminal variable region of nCLP2 are also involved in HMW multimer formation, the mutant protein nCLP2-C29/33S, in which both Cys-29 and Cys-33 in the N-terminal variable region were substituted with serine residues, was subjected to gel filtration chromatography. Adipo-C39S, the adiponectin mutant in which the Cys-39 in the N-terminal variable region was

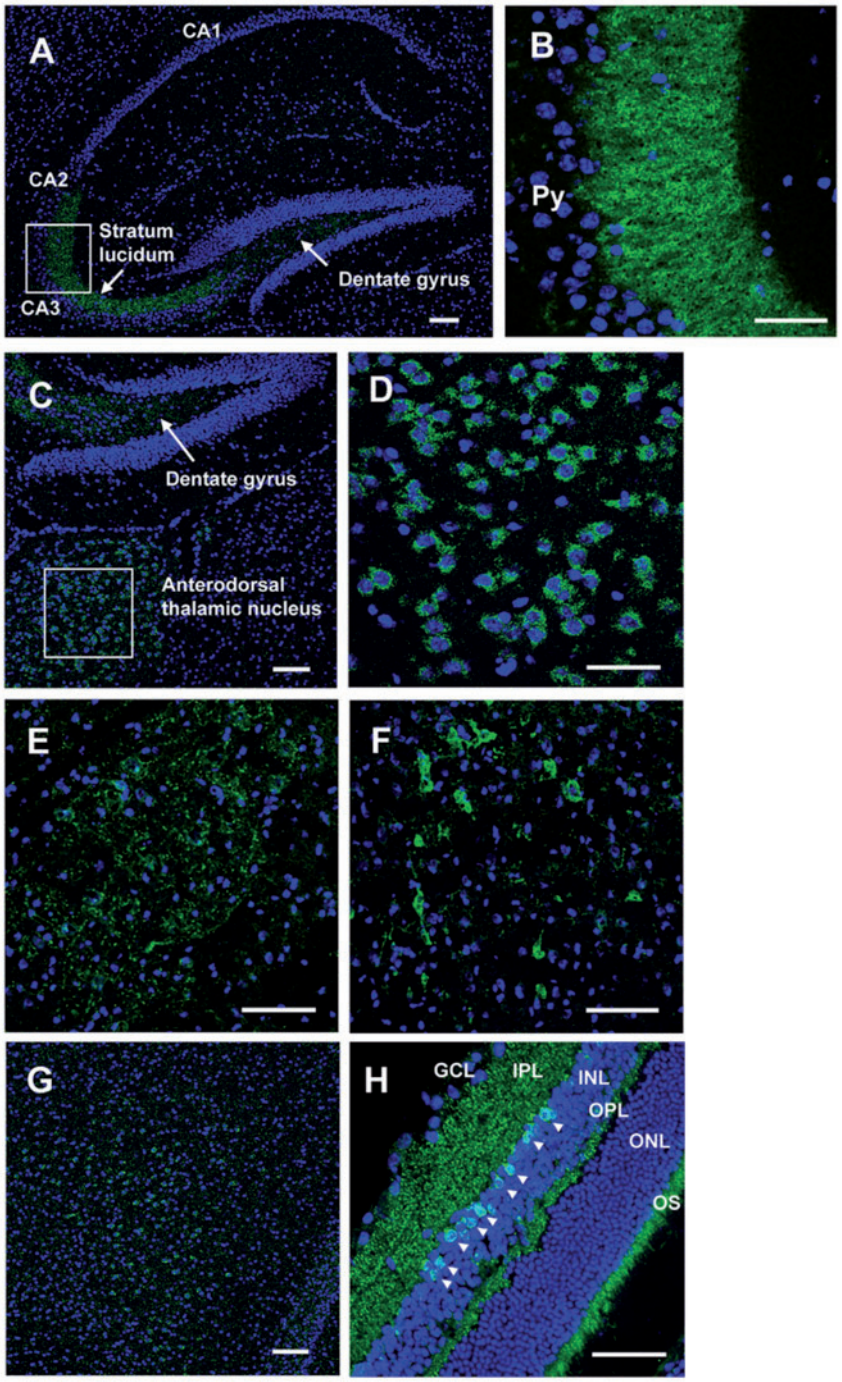

Fig. 5 Immunohistochemical detection of nCLP2 in adult brain and eye. Sagittal cryosections of a 9-week-old mouse brain and retina were immunostained with anti-nCLP2-S antibody (green) and counterstained with Hoechst 33342 (blue) to visualize nuclei. In the hippocampus, nCLP2 was detected in the dentate gyrus and stratum lucidum of the CA3 region but not in other regions including the pyramidal cell layer (A). (B) Shows the magnified view of the boxed area in (A). nCLP2 signals were also detected in soma and/or neurites of neurons in the anterodorsal thalamic nucleus (C), red nucleus (E), inferior olivary nucleus (F) and entorhinal cortex (G). (D) Shows the magnified view of the boxed area in (C). In the eye, nCLP2 signals were restricted to the retina, where inner and outer plexiform layers (IPL and OPL) and amacrine cells (white arrowheads) in the inner nuclear layer (INL) were selectively stained with the antibodies (H). Signals present in the outer segment of the photoreceptor layer (OS) in (H) were non-specific, as fluorescence-labelled secondary antibodies alone stained this region in the retina. GCL, ganglion cell layer; ONL, outer nuclear layer. Py, pyramidal cell layer. The bar represents 100 μm in (A, C and E–G) and 50 μm in (B, D and H).

substituted with serine, was also subjected to gel filtration as a control. Adipo-C39S eluted essentially as a single peak at the trimer position (Fig. 8C), consistent with a previous report (*6*). Similarly, nCLP2-C29/33S gave a major peak corresponding to the trimer position almost equivalent to that of the adiponectin trimer, although a weaker peak was also detected at the position of the hexamer (Fig. 8D). These results are consistent with the scheme that trimeric protomers of nCLP2 are assembled into HMW multimers through inter-trimer disulphide bonds involving two cysteine residues in the N-terminal variable region, as has

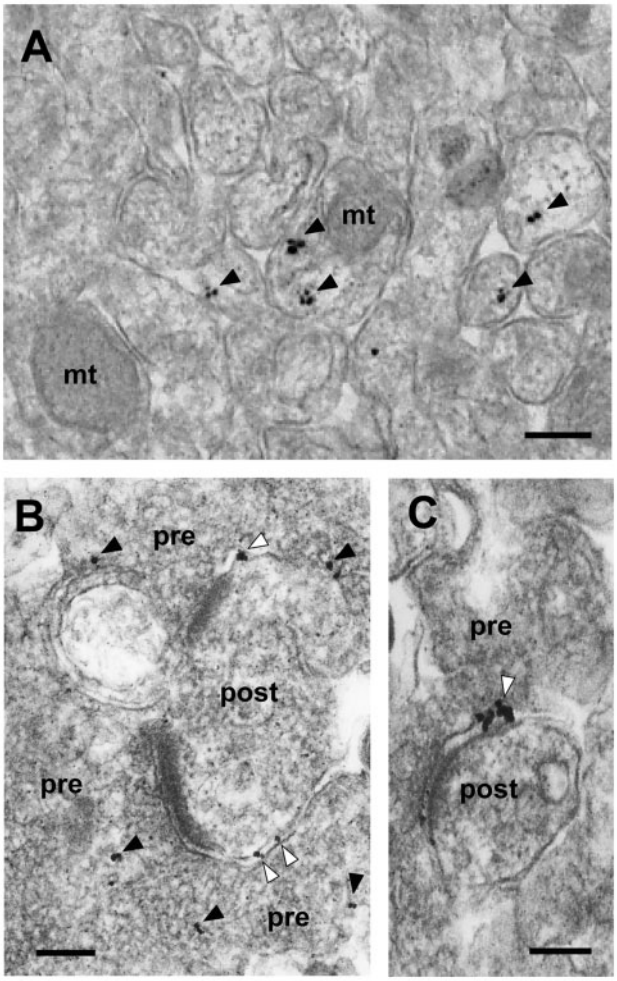

Fig. 6 Immunoelectron microscopic localization of nCLP2 in the stratum lucidum of the hippocampus. Ultrathin sections of the hippocampus from a 9-week-old mouse were immunostained with anti-nCLP2-S, followed by labelling with gold particle-conjugated secondary antibodies. nCLP2 signals (arrowheads) were detected in mossy fibre bundles, as shown in the axial section of the mossy fibre bundles (A). nCLP2 signals were also detected in the synaptic clefts between synaptic boutons and dendritic spines of the CA3 pyramidal cells (B and C). Signals in the synaptic clefts are denoted by open arrowheads. The bars represent 200 nm. mt, mitochondria; pre, presynapse; post, postsynapse.

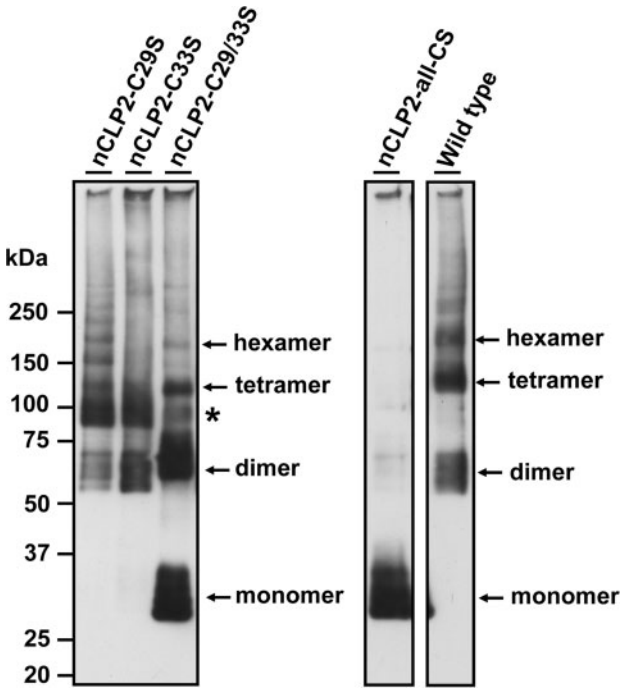

Fig. 7 Immunoblot analysis of nCLP2 and its mutants. Conditioned media of 293F cells transfected with nCLP2 and its mutants (nCLP2-C29S, nCLP2-C33S, nCLP2-C29/33S, and nCLP2-all-CS, in which Cys-29, Cys-33, both Cys-29 and Cys-33, and all cysteine residues were substituted with serine residues) were subjected to SDS–PAGE on 5–20% gradient gels under non-reducing conditions, followed by immunoblotting with an anti-FLAG antibody. Bands corresponding to monomer, dimer, trimer, tetramer and hexamer are indicated on the right. Monomers were detected with nCLP2-C29/33S and nCLP2-all-CS, but not nCLP2-C29S and nCLP2-C33S. The trimer was detected in nCLP2-C29S and nCLP2-C33S. The asterisk points to the position corresponding to the trimer.

been demonstrated for the multimer formation of adiponectin.

To corroborate this scheme, both Adipo-C39S and nCLP2-C29/33S were subjected to chemical crosslinking using the homobifunctional crosslinker BS^3. SDS–PAGE under reducing conditions showed that adipo-C39S predominantly gave rise to trimers upon titration with increasing concentration of BS^3 (Fig. 9). Similarly, nCLP2-C29/33S also yielded trimers as the major crosslinked product, although hexameric and oligomeric forms of the crosslinked products were also detected at >1 mM BS^3. These results are consistent with the scheme that nCLP2, like adiponectin, assembles into multimers via trimeric protomers, and two cysteine residues in the N-terminal variable region contribute to stabilize the multimers by inter-trimer disulphide bonds.

Discussion

A hallmark of C1q family proteins is trimer formation of their protomers (*3*). The trimers often assemble into disulphide-linked hexamers and/or HMW multimers. The prototypic complement C1q protein forms an 18-mer comprising six heterotrimers of the A, B and C chains, adopting the overall shape of a bouquet of tulips (*3*). Adiponectin forms heterogenous oligomers, including trimers, hexamers and HMW multimers (*6*, *28*, *34*). Trimer formation of C1q family proteins is driven by their gC1q and collagenous domains, both of which have the intrinsic capability to assemble into trimers (*35–37*), although not all C1q family proteins contain the collagenous domain. Mutations that cause amino acid substitution in the gC1q domain have been shown to impair trimer formation of adiponectin (*6*) and collagen X (*7*,*38*), resulting in reduced expression and/or secretion (*6*, *39*). Given the presence of both gC1q and collagenous domains in nCLP2, it is conceivable that nCLP2 also forms a trimer, which in turn assembles into HMW multimers, as schematically depicted in Fig. 10. The resulting multimers are stabilized by interchain disulphide bonds primarily involving the cysteine residues in the N-terminal

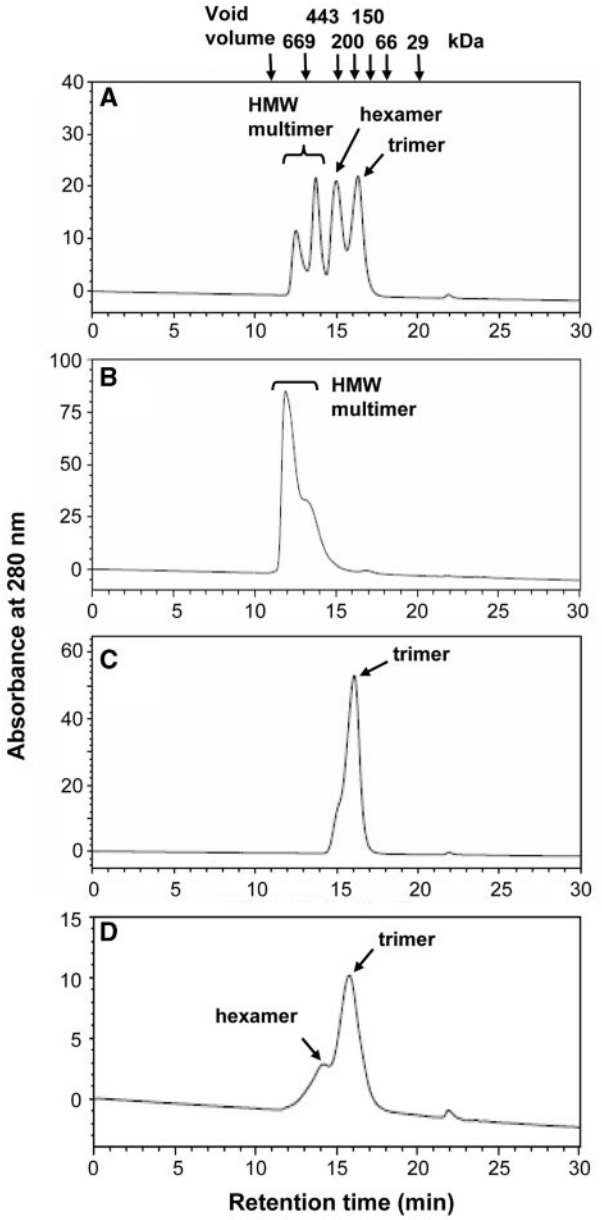

Fig. 8 Gel filtration chromatography of adiponectin, nCLP2 and their mutants. Adiponectin (A), nCLP2 (B) and their mutants, adiponectin-C39S (C) and nCLP2-C29/33S (D), of which cysteine residues in the N-terminal variable regions were substituted with serine residues, were purified from conditioned media of transfected 293F cells and subjected to gel filtration chromatography. Elution positions of molecular mass markers are indicated at the top of the figure. The peaks corresponding to trimers, hexamers and HMW multimers are assigned based on the elution positions of adiponectin and its mutant. Ordinates are expressed in milliabsorbance units.

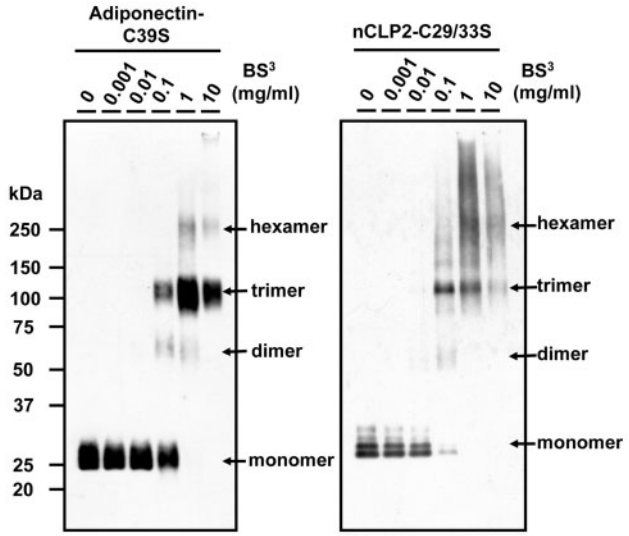

Fig. 9 Chemical crosslinking of nCLP2-C29/33S and adiponectin-C39S. nCLP2-C29/33S and adiponectin-C39S (10 μg/ml) were incubated with increasing concentrations of the homobifunctional crosslinker BS^3 for 30 min. The crosslinked products were subjected to SDS–PAGE on 5–20% gradient gels under reducing conditions, followed by immunoblotting with an anti-FLAG antibody. The bands corresponding to monomer, dimer, trimer and hexamer are assigned based on the band patterns of crosslinked products of adiponectin and its mutant. Note that trimers were detected not only with adiponectin-C39S but also with nCLP2-C29/33S following crosslinking.

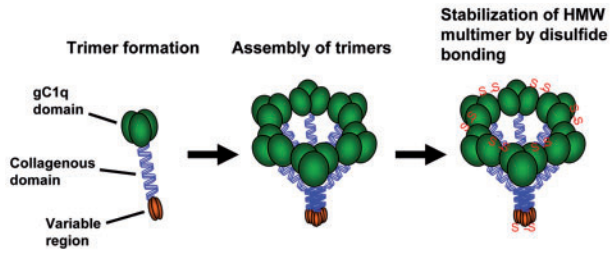

Fig. 10 Schematic model of the multimer formation of nCLP2. nCLP2 protomers assemble into trimers through self-association of the collagenous and gC1q domains. The trimers further assemble into multimers through lateral association of the collagen triple helices or the interaction between trimerized gC1q domains. The resulting multimers are stabilized by the inter-trimer disulphide bonds at the N-terminal variable region. The cysteine residues in the gC1q domain also contribute to the stabilization of the multimers by forming disulphide bonds between trimerized gC1q domains.

variable region. In support of this scheme, nCLP2-C29/33S, the nCLP2 mutant with substitution of two cysteine residues with serine in the N-terminal variable region, was predominantly eluted at the position of trimers upon gel filtration chromatography, whereas intact nCLP2 was eluted as HMW multimers with an apparent mass of >700 kDa. Further support for this scheme was obtained by chemical crosslinking experiments, in which nCLP2-C29/33S gave rise to a covalently linked trimer upon titration with increasing concentrations of the crosslinker BS^3.

The importance of the interchain disulphide bonds at the N-terminal variable region in stable multimer formation has been demonstrated with adiponectin. The adiponectin mutant Adipo-C39S, in which a serine residue was substituted for Cys-39, behaved as a trimer in velocity sedimentation and gel filtration chromatography, whereas intact adiponectin gave peaks corresponding to a hexamer and HMW multimers (*34*; also this study). Consistent with the importance of the N-terminal disulphide bonds in multimer

formation of nCLP2 and adiponectin, the complement C1q protein gives rise to an 18-mer assembled from three hexamers that are comprised of three disulphide-linked dimers (*i.e.* two A–B dimers and a C–C dimer) through the cysteine residues in the N-terminal region (*3*). Given the occurrence of cysteine residue(s) in the N-terminal regions of 'most C1q family proteins' including Cblns (*32*) and C1qTNF9 (*40*), the N-terminally located cysteine residues may well be generally involved in multimer formation of C1q family proteins. This situation is analogous to the collectin family of proteins that also undergoes multimerization via the assembly of trimeric units, in which the cysteine residues in the N-terminal region are involved in disulphide-bonded multimer formation (*41*). SDS–PAGE under non-reducing conditions showed that all nCLP2 protomers are disulphide-linked to produce a dimer, a tetramer and HMW oligomers. nCLP2 differs from adiponectin and the complement C1q in that it possesses two cysteine residues in the N-terminal variable region. Both cysteine residues seem to participate in interchain disulphide bonds, since only the nCLP2 mutant in which both Cys-29 and Cys-33 were substituted with serine residues, but not those bearing single substitution at either residue, yielded a monomer in SDS–PAGE under non-reducing conditions. It should be noted, however, that nCLP2-C29/33S gave not only the monomer band but also bands corresponding to a dimer and a tetramer, indicating that the cysteine residues other than those in the N-terminal region are involved in interchain disulphide bonds.

nCLP2 contains four cysteine residues, two in the N-terminal variable region and two in the gC1q domain. It is conceivable, therefore, that the cysteine residues in the gC1q domain also participate, at least in part, in interchain disulphide bonds, yielding dimer and tetramer bands when nCLP2-C29/33S was subjected to SDS–PAGE under non-reducing conditions. Consistent with this conclusion, gel filtration chromatography showed that a fraction of nCLP2-C29/33S was eluted at the hexamer position, an indicative of an inter-trimer disulphide bond involving cysteine residues other than those in the N-terminal region. It is interesting to note that nCLP2, unlike other C1q family proteins, contains two cysteine residues, Cys-197 and Cys-224, in the gC1q domain. Of these, Cys-197 is conserved among other C1q family proteins. Crystallographic analyses of the gC1q domain of some C1q family proteins revealed that the conserved cysteine residue is situated to comprise the hydrophobic core buried within the domain (*4*, *35*, *42*, *43*), making it likely that Cys-224, but not Cys-197, participates in the disulphide-linked hexamer formation, although we cannot exclude a minor contribution of Cys-197 to the disulphide bond(s) linking of two trimers. Superimposition of Cys-197 and Cys-224 onto the gC1q domain of the complement C1q protein whose three-dimensional structures have been determined by X-ray crystallography (*35*) indicates that both Cys-197 and Cys-224 are positioned at the periphery of the trimerized gC1q domain (Supplementary Fig. S5) and, therefore, inaccessible to each other to form intra-trimer disulphide bonds, consistent with the conclusion that the cysteine residues in the gC1q domain participate in inter-trimer disulphide bonds yielding a hexamer.

Our *in situ* hybridization and immunohistochemical analyses revealed a restricted expression of nCLP2 in the CNS. In the hippocampus, nCLP2 is expressed in dentate granule cells and localized at the stratum lucidum, to which the mossy fibre axons of granule cells project. Immunoelectron microscopy localized nCLP2 in mossy fibres and presynaptic boutons and at the synaptic clefts between synaptic boutons and dendritic spines of CA3 pyramidal cells. These results imply that nCLP2 expressed in granule cells is anterogradely transported in mossy fibres and secreted from the presynaptic termini to the synaptic clefts. Since the termini of mossy fibres are known to contact the thorny excrescences of CA3 pyramidal cells, it seems likely that nCLP2 released from presynaptic termini of the granule cells impacts on their postsynaptic target, CA3 pyramidal neurons, through interaction with its putative receptor(s) on the dendritic spines of the pyramidal neurons. However, the molecular identity of the putative receptor(s) remains unexplored. Similar anterograde transport has been reported for brain-derived neurotrophic factor (BDNF), which is expressed in the granule cells, transported in the mossy fibres, and released towards the synaptic clefts (*44*, *45*). The released BDNF acts on the receptors on the presynapses (*46*) and postsynaptic spines of dendrites of CA3 pyramidal cells (*47–49*), thereby inducing long-term potentiation of synaptic transmission through regulation of the integrity and plasticity of the synapses. Our results also show that nCLP2 is localized in the neurons of entorhinal cortex, anterodorsal thalamic nucleus, red nucleus and inferior olivary nucleus. The entorhinal-dentate-hippocampal system is a major neuronal network involved in the long-term memory formation (*50*, *51*). The anterodorsal thalamic nucleus also participates in memory formation as a part of Papez's circuit (*52–55*). Red nucleus and inferior nucleus are connected to each other and comprise a part of the neuronal network associated with motor functions (*56*, *57*). It is tempting to speculate that nCLP2 expressed in these brain regions is also anterogradely transported through the axons towards presynaptic termini and released from synaptic boutons to synaptic clefts, where nCLP2 binds to putative receptor(s) on pre- and/or postsynapses, and modulates synaptic plasticity and integrity in the neuronal networks related to memory formation, although further studies are needed to explore this possibility. Immunohistochemical signals for nCLP2 were diffuse and not discernible in these brain regions, except for the signals in cell bodies. This is in striking contrast to the immunohistochemical detection of nCLP2 expressed in hippocampal granule cells; nCLP2 was clearly detected in the stratum lucidum of CA3 region, where mossy fibres form tight bundles and possess huge synaptic boutons, but not in the cell bodies of hippocampal granule cells. High density of mossy fibres and the resulting synapses should facilitate the immunohistochemical detection

of nCLP2 in the stratum lucidum of CA3 region, while nCLP2-expressing cells and their axons are sparse in other brain regions, *e.g.* anterodorsal thalamic nucleus, making it difficult to detect the nCLP2 proteins transported through axons and secreted from the synaptic termini. It should be noted that nCLP2 is also expressed in retina and localized in the inner and outer plexiform layers, where neurons of the internal and external granular layers extend their neurites towards ganglion cells or neurons of the internal granular layer and form numerous synapses. nCLP2 expressed in the neurons of internal and external granular layers may also be transported through the neurites and secreted towards synaptic clefts between presynapses and dendritic spines of ganglion cells or neurons of the internal granular layer, as expected for its anterograde transport in the hippocampus.

nCLP2 is expressed in the adult brain and the embryonic brain after embryonic day 12 in mice. The constitutive expression in the brain implies that nCLP2 plays a role not only in developmental synaptic formation but also in the maintenance of synaptic contacts and regulation of synaptic plasticity and integrity. In this context, it is interesting to note that Cbln1, another C1q family protein expressed in the brain, has been reported to play an essential role in integrity and plasticity of the granule cell-Purkinje cell synapses in the cerebellum (*13*). Cbln1 is a unique synapse organizer that is required not only for the normal development of parallel fibre–Purkinje cell synapses but also for their maintenance in the mature cerebellum (*58*). The chronic activation of cerebellar granule cells by elevating extracellular K^+ levels or by adding kainate downregulates the expression of Cbln1 mRNA, resulting in the reduction of the number of excitatory synapses on Purkinje cell dendrites. The activity-dependent regulation of Cbln1 expression is considered as a presynaptic mechanism by which parallel fibre-Purkinje cell synapses adapt to neuronal activity, thereby maintaining homeostasis of synapse organization (*59*). Since nCLP2 is expressed in hippocampal granule cells and localized in excitatory synapses of mossy fibres, nCLP2 may also be involved in the regulation of synaptic plasticity and integrity in a neuronal activity-dependent manner.

In this study, we found three other C1q family proteins sharing high sequence homologies with nCLP2. RT-PCR analyses demonstrated that nCLP1 and nCLP3, like nCLP2, are selectively expressed in CNS tissues including brain, spinal cord and eye, although nCLP4 transcripts were detected not only in the CNS tissues but also in other tissues. Although the function and oligomeric states of the other nCLPs remain to be explored, they may also be secreted from presynaptic termini towards target neurons as homo and/or hetero-multimers. nCLPs share very high sequence homologies in their gC1q domains, where C1q family proteins recognize interacting partners to trimerize (*60*). The gC1q domains of three chains of the complement C1q have been shown to assemble into a heterotrimer (*35*). Given the high sequence homologies in their gC1q domains, nCLPs may also be capable of assembling into heterotrimers. Consistent with this possibility, nCLP1, also designated C1q-related factor, has been shown to be expressed in the inferior olivary nucleus and red nucleus (*16*), where nCLP2 is also expressed. Our preliminary immunohistochemical studies showed that nCLP1 and nCLP3 were also localized in the inner and outer plexiform layers of the retina (data not shown), consistent with the possibility that nCLP1–3 form heterotrimers. In support of this possibility, nCLP2 was found to yield heterocomplexes with nCLP1 and nCLP3 (Shimono, C., unpublished observation). The potential hetero-multimerization may contribute to the functional diversity of nCLPs and regulate the binding affinity and/or selectivity towards their putative receptor(s), providing a regulatory mechanism of nCLP function in maintenance and/or integrity of neuronal networks. Further studies exploring their tissue localization, molecular properties including the mechanism of multimer formation and identification of their putative receptor(s) should unravel their roles in synaptic function and maintenance in the CNS.

Acknowledgements

The authors thank Dr Sadao Shiosaka (Nara Advanced Institute of Science and Technology) for his invaluable advice on immunoelectron microscopy. They also thank Minoru Fukayama (Central Research Laboratories, Aichi Medical University) for his assistance in the matrix-assisted laser desorption ionization time-of-flight mass spectrometry and gel filtration chromatography and Yousuke Ishihara (Hanaichi UltraStructure Research Institute, Hanaichi Co., Ltd.) for his assistance in immunoelectron microscopic analyses.

Supplementary data

Supplementary Data are available at *JB* Online.

Funding

The Ministry of Education, Culture, Sports, Science and Technology of Japan, for RIKEN Omics Science Center.

Conflict of interest

None declared.

References

1. Ghai, R., Waters, P., Roumenina, L.T., Gadjeva, M., Kojouharova, M.S., Reid, K.B., Sim, R.B., and Kishore, U. (2007) C1q and its growing family. *Immunobiology* **212**, 253–266
2. Tang, Y.T., Hu, T., Arterburn, M., Boyle, B., Bright, J.M., Palencia, S., Emtage, P.C., and Funk, W.D. (2005) The complete complement of C1q-domain-containing proteins in Homo sapiens. *Genomics* **86**, 100–111
3. Kishore, U., Gaboriaud, C., Waters, P., Shrive, A.K., Greenhough, T.J., Reid, K.B., Sim, R.B., and Arlaud, G.J. (2004) C1q and tumor necrosis factor superfamily: modularity and versatility. *Trends Immunol.* **25**, 551–561
4. Shapiro, L. and Scherer, P.E. (1998) The crystal structure of a complement-1q family protein suggests an evolutionary link to tumor necrosis factor. *Curr. Biol.* **8**, 335–338
5. Radjainia, M., Wang, Y., and Mitra, A.K. (2008) Structural polymorphism of oligomeric adiponectin visualized by electron microscopy. *J. Mol. Biol.* **381**, 419–430

6. Waki, H., Yamauchi, T., Kamon, J., Ito, Y., Uchida, S., Kita, S., Hara, K., Hada, Y., Vasseur, F., Froguel, P., Kimura, S., Nagai, R., and Kadowaki, T. (2003) Impaired multimerization of human adiponectin mutants associated with diabetes. Molecular structure and multimer formation of adiponectin. *J. Biol. Chem.* **278**, 40352–40363
7. Bateman, J.F., Freddi, S., McNeil, R., Thompson, E., Hermanns, P., Savarirayan, R., and Lamandé, S.R. (2004) Identification of four novel COL10A1 missense mutations in schmid metaphyseal chondrodysplasia: further evidence that collagen X NC1 mutations impair trimer assembly. *Hum. Mutat.* **23**, 396
8. Kishore, U. and Reid, K.B. (2000) C1q: structure, function, and receptors. *Immunopharmacology* **49**, 159–170
9. Kadowaki, T. and Yamauchi, T. (2005) Adiponectin and adiponectin receptors. *Endocr. Rev.* **26**, 439–451
10. Kondo, H., Shimomura, I., Matsukawa, Y., Kumada, M., Takahashi, M., Matsuda, M., Ouchi, N., Kihara, S., Kawamoto, T., Sumitsuji, S., Funahashi, T., and Matsuzawa, Y. (2002) Association of adiponectin mutation with type 2 diabetes: a candidate gene for the insulin resistance syndrome. *Diabetes* **51**, 2325–2328
11. Akiyama, H., Furukawa, S., Wakisaka, S., and Maeda, T. (2006) Cartducin stimulates mesenchymal chondroprogenitor cell proliferation through both extracellular signal-regulated kinase and phosphatidylinositol 3-kinase/Akt pathways. *FEBS J.* **273**, 2257–2263
12. Zacchigna, L., Vecchione, C., Notte, A., Cordenonsi, M., Dupont, S., Maretto, S., Cifelli, G., Ferrari, A., Maffei, A., Fabbro, C., Braghetta, P., Marino, G., Selvetella, G., Aretini, A., Colonnese, C., Bettarini, U., Russo, G., Soligo, S., Adorno, M., Bonaldo, P., Volpin, D., Piccolo, S., Lembo, G., and Bressan, G.M. (2006) Emilin1 links TGF-beta maturation to blood pressure homeostasis. *Cell* **124**, 929–942
13. Hirai, H., Pang, Z., Bao, D., Miyazaki, T., Li, L., Miura, E., Parris, J., Rong, Y., Watanabe, M., Yuzaki, M., and Morgan, J.I. (2005) Cbln1 is essential for synaptic integrity and plasticity in the cerebellum. *Nat. Neurosci.* **8**, 1534–1541
14. Miura, E., Iijima, T., Yuzaki, M., and Watanabe, M. (2006) Distinct expression of Cbln family mRNAs in developing and adult mouse brains. *Eur. J. Neurosci.* **24**, 750–760
15. Yuzaki, M. (2008) Cbln and C1q family proteins: new transneuronal cytokines. *Cell Mol. Life Sci.* **65**, 1698–1705
16. Bérubé, N.G., Swanson, X.H., Bertram, M.J., Kittle, J.D., Didenko, V., Baskin, D.S., Smith, J.R., and Pereira-Smith, O.M. (1999) Cloning and characterization of CRF, a novel C1q-related factor, expressed in areas of the brain involved in motor function. *Brain Res. Mol. Brain Res.* **63**, 233–240
17. Kubota, N., Yano, W., Kubota, T., Yamauchi, T., Itoh, S., Kumagai, H., Kozono, H., Takamoto, I., Okamoto, S., Shiuchi, T., Suzuki, R., Satoh, H., Tsuchida, A., Moroi, M., Sugi, K., Noda, T., Ebinuma, H., Ueta, Y., Kondo, T., Araki, E., Ezaki, O., Nagai, R., Tobe, K., Terauchi, Y., Ueki, K., Minokoshi, Y., and Kadowaki, T. (2007) Adiponectin stimulates AMP-activated protein kinase in the hypothalamus and increases food intake. *Cell Metab.* **6**, 55–68
18. Miller, G. (2007) Neurobiology. Immune molecules prune synapses in developing brain. *Science* **318**, 1710–1711
19. Fourgeaud, L. and Boulanger, L.M. (2007) Synapse remodeling, compliments of the complement system. *Cell* **131**, 1034–1036
20. Manabe, R., Tsutsui, K., Yamada, T., Kimura, M., Nakano, I., Shimono, C., Sanzen, N., Furutani, Y., Fukuda, T., Oguri, Y., Shimamoto, K., Kiyozumi, D., Sato, Y., Sado, Y., Senoo, H., Yamashina, S., Fukuda, S., Kawai, J., Sugiura, N., Kimata, K., Hayashizaki, Y., and Sekiguchi, K. (2008) Transcriptome-based systematic identification of extracellular matrix proteins. *Proc. Natl Acad. Sci. USA* **105**, 12849–12854
21. Okazaki, Y., Furuno, M., Kasukawa, T., Adachi, J., Bono, H., Kondo, S., Nikaido, I., Osato, N., Saito, R., Suzuki, H., Yamanaka, I., Kiyosawa, H., Yagi, K., Tomaru, Y., Hasegawa, Y., Nogami, A., Schonbach, C., Gojobori, T., Baldarelli, R., Hill, D.P., Bult, C., Hume, D.A., Quackenbush, J., Schriml, L.M., Kanapin, A., Matsuda, H., Batalov, S., Beisel, K.W., Blake, J.A., Bradt, D., Brusic, V., Chothia, C., Corbani, L.E., Cousins, S., Dalla, E., Dragani, T.A., Fletcher, C.F., Forrest, A., Frazer, K.S., Gaasterland, T., Gariboldi, M., Gissi, C., Godzik, A., Gough, J., Grimmond, S., Gustincich, S., Hirokawa, N., Jackson, I.J., Jarvis, E.D., Kanai, A., Kawaji, H., Kawasawa, Y., Kedzierski, R.M., King, B.L., Konagaya, A., Kurochkin, I.V., Lee, Y., Lenhard, B., Lyons, P.A., Maglott, D.R., Maltais, L., Marchionni, L., McKenzie, L., Miki, H., Nagashima, T., Numata, K., Okido, T., Pavan, W.J., Pertea, G., Pesole, G., Petrovsky, N., Pillai, R., Pontius, J.U., Qi, D., Ramachandran, S., Ravasi, T., Reed, J.C., Reed, D.J., Reid, J., Ring, B.Z., Ringwald, M., Sandelin, A., Schneider, C., Semple, C.A., Setou, M., Shimada, K., Sultana, R., Takenaka, Y., Taylor, M.S., Teasdale, R.D., Tomita, M., Verardo, R., Wagner, L., Wahlestedt, C., Wang, Y., Watanabe, Y., Wells, C., Wilming, L.G., Wynshaw-Boris, A., Yanagisawa, M., Yang, I., Yang, L., Yuan, Z., Zavolan, M., Zhu, Y., Zimmer, A., Carninci, P., Hayatsu, N., Hirozane-Kishikawa, T., Konno, H., Nakamura, M., Sakazume, N., Sato, K., Shiraki, T., Waki, K., Kawai, J., Aizawa, K., Arakawa, T., Fukuda, S., Hara, A., Hashizume, W., Imotani, K., Ishii, Y., Itoh, M., Kagawa, I., Miyazaki, A., Sakai, K., Sasaki, D., Shibata, K., Shinagawa, A., Yasunishi, A., Yoshino, M., Waterston, R., Lander, E.S., Rogers, J., Birney, E., and Hayashizaki, Y. FANTOM Consortium, RIKEN Genome Exploration Research Group Phase I & II Team. (2002) Analysis of the mouse transcriptome based on functional annotation of 60,770 full-length cDNAs. *Nature* **420**, 563–573
22. Nakai, K. and Horton, P. (1999) PSORT: a program for detecting the sorting signals of proteins and predicting their subcellular localization. *Trends Biochem. Sci.* **24**, 34–35
23. Hirokawa, T., Boon-Chieng, S., and Mitaku, S. (1998) SOSUI: classification and secondary structure prediction system for membrane proteins. *Bioinformatics* **14**, 378–379
24. Pearson, W.R. (2000) Flexible sequence similarity searching with the FASTA3 program package. *Methods Mol. Biol.* **132**, 185–219
25. Furutani, Y., Manabe, R., Tsutsui, K., Yamada, T., Sugimoto, N., Fukuda, S., Kawai, J., Sugiura, N., Kimata, K., Hayashizaki, Y., and Sekiguchi, K. (2005) Identification and characterization of photomedins: novel olfactomedin-domain-containing proteins with chondroitin sulphate-E-binding activity. *Biochem. J.* **389**, 675–684
26. Laemmli, U.K. (1970) Cleavage of structural proteins during the assembly of the head of bacteriophage T4. *Nature* **227**, 680–685

27. Shimizu, T., Kagawa, T., Wada, T., Muroyama, Y., Takada, S., and Ikenaka, K. (2005) Wnt signaling controls the timing of oligodendrocyte development in the spinal cord. *Dev. Biol.* **282**, 397–410
28. Tsao, T.S., Tomas, E., Murrey, H.E., Hug, C., Lee, D.H., Ruderman, N.B., Heuser, J.E., and Lodish, H.F. (2003) Role of disulfide bonds in Acrp30/adiponectin structure and signaling specificity. Different oligomers activate different signal transduction pathways. *J. Biol. Chem.* **278**, 50810–50817
29. Wang, Y., Lam, K.S., Chan, L., Chan, K.W., Lam, J.B., Lam, M.C., Hoo, R.C., Mak, W.W., Cooper, G.J., and Xu, A. (2006) Posttranslational modifications on the four conserved lysine residues within the collagenous domain of adiponectin are required for the formation of its high-molecular-weight oligomeric complex. *J. Biol. Chem.* **281**, 16391–16400
30. Richards, A.A., Stephens, T., Charlton, H.K., Jones, A., Macdonald, G.A., Prins, J.B., and Whitehead, J.P. (2006) Adiponectin multimerization is dependent on conserved lysines in the collagenous domain: evidence for regulation of multimerization by alterations in post-translational modifications. *Mol. Endocrinol.* **20**, 1673–1687
31. Colley, K.J. and Baenziger, J.U. (1987) Identification of the post-translational modifications of the core-specific lectin. The core-specific lectin contains hydroxyproline, hydroxylysine, and glucosylgalactosylhydroxylysine residues. *J. Biol. Chem.* **262**, 10290–10295
32. Bao, D., Pang, Z., and Morgan, J.I. (2005) The structure and proteolytic processing of Cbln1 complexes. *J. Neurochem.* **95**, 618–629
33. Tsao, T.S., Murrey, H.E., Hug, C., Lee, D.H., and Lodish, H.F. (2002) Oligomerization state-dependent activation of NF-kappa B signaling pathway by adipocyte complement-related protein of 30 kDa (Acrp30). *J. Biol. Chem.* **277**, 29359–29362
34. Pajvani, U.B., Du, X., Combs, T.P., Berg, A.H., Rajala, M.W., Schulthess, T., Engel, J., Brownlee, M., and Scherer, P.E. (2003) Structure-function studies of the adipocyte-secreted hormone Acrp30/adiponectin. Implications for metabolic regulation and bioactivity. *J. Biol. Chem.* **278**, 9073–9085
35. Gaboriaud, C., Juanhuix, J., Gruez, A., Lacroix, M., Darnault, C., Pignol, D., Verger, D., Fontecilla-Camps, J.C., and Arlaud, G.J. (2003) The crystal structure of the globular head of complement protein C1q provides a basis for its versatile recognition properties. *J. Biol. Chem.* **278**, 46974–46982
36. Zhang, Y. and Chen, Q. (1999) The noncollagenous domain 1 of type X collagen. A novel motif for trimer and higher order multimer formation without a triple helix. *J. Biol. Chem.* **274**, 22409–22413
37. Beck, K. and Brodsky, B. (1998) Supercoiled protein motifs: the collagen triple-helix and the alpha-helical coiled coil. *J. Struct. Biol.* **122**, 17–29
38. Chan, D., Cole, W.G., Rogers, J.G., and Bateman, J.F. (1995) Type X collagen multimer assembly *in vitro* is prevented by a Gly618 to Val mutation in the alpha 1(X) NC1 domain resulting in Schmid metaphyseal chondrodysplasia. *J. Biol. Chem.* **270**, 4558–4562
39. Bateman, J.F., Wilson, R., Freddi, S., Lamandé, S.R., and Savarirayan, R. (2005) Mutations of COL10A1 in Schmid metaphyseal chondrodysplasia. *Hum. Mutat.* **25**, 525–534
40. Wong, G.W., Krawczyk, S.A., Kitidis-Mitrokostas, C., Ge, G., Spooner, E., Hug, C., Gimeno, R., and Lodish, H.F. (2009) Identification and characterization of CTRP9, a novel secreted glycoprotein, from adipose tissue that reduces serum glucose in mice and forms heterotrimers with adiponectin. *FASEB J.* **23**, 241–258
41. van de Wetering, J.K., van Golde, L.M., and Batenburg, J.J. (2004) Collectins: players of the innate immune system. *Eur. J. Biochem.* **271**, 1229–1249
42. Kvansakul, M., Bogin, O., Hohenester, E., and Yayon, A. (2003) Crystal structure of collagen alpha1(VIII) NC1 trimer. *Matrix Biol.* **22**, 145–152
43. Bogin, O., Kvansakul, M., Rom, E., Singer, J., Yayon, A., and Hohenester, E. (2002) Insight into Schmid metaphyseal chondrodysplasia from the crystal structure of the collagen X NC1 domain trimer. *Structure* **10**, 165–173
44. Dieni, S. and Rees, S. (2002) Distribution of brain-derived neurotrophic factor and TrkB receptor proteins in the fetal and postnatal hippocampus and cerebellum of the guinea pig. *J. Comp. Neurol.* **454**, 229–240
45. Smith, M.A., Zhang, L.X., Lyons, W.E., and Mamounas, L.A. (1997) Anterograde transport of endogenous brain-derived neurotrophic factor in hippocampal mossy fibres. *Neuroreport* **8**, 1829–1834
46. Gómez-Palacio-Schjetnan, A. and Escobar, M.L. (2008) *In vivo* BDNF modulation of adult functional and morphological synaptic plasticity at hippocampal mossy fibres. *Neurosci. Lett.* **445**, 62–67
47. Danzer, S.C. and McNamara, J.O. (2004) Localization of brain-derived neurotrophic factor to distinct terminals of mossy fibre axons implies regulation of both excitation and feedforward inhibition of CA3 pyramidal cells. *J. Neurosci.* **24**, 11346–11355
48. Goodman, L.J., Valverde, J., Lim, F., Geschwind, M.D., Federoff, H.J., Geller, A.I., and Hefti, F. (1996) Regulated release and polarized localization of brain-derived neurotrophic factor in hippocampal neurons. *Mol. Cell Neurosci.* **7**, 222–238
49. Zagrebelsky, M., Holz, A., Dechant, G., Barde, Y.A., Bonhoeffer, T., and Korte, M. (2005) The p75 neurotrophin receptor negatively modulates dendrite complexity and spine density in hippocampal neurons. *J. Neurosci.* **25**, 9989–9999
50. Bartesaghi, R., Raffi, M., and Ciani, E. (2006) Effect of early isolation on signal transfer in the entorhinal cortex-dentate-hippocampal system. *Neuroscience* **137**, 875–890
51. Bartesaghi, R., Migliore, M., and Gessi, T. (2006) Input-output relations in the entorhinal cortex-dentate-hippocampal system: evidence for a non-linear transfer of signals. *Neuroscience* **142**, 247–265
52. Warburton, E.C., Baird, A.L., and Aggleton, J.P. (1997) Assessing the magnitude of the allocentric spatial deficit associated with complete loss of the anterior thalamic nuclei in rats. *Behav. Brain Res.* **87**, 223–232
53. Sziklas, V. and Petrides, M. (2007) Contribution of the anterior thalamic nuclei to conditional learning in rats. *Hippocampus* **17**, 456–461
54. Vertes, R.P., Albo, Z., and Viana Di Prisco, G. (2001) Theta-rhythmically firing neurons in the anterior thalamus: implications for mnemonic functions of Papez's circuit. *Neuroscience* **104**, 619–625
55. Warburton, E.C., Baird, A.L., Morgan, A., Muir, J.L., and Aggleton, J.P. (2000) Disconnecting hippocampal projections to the anterior thalamus produces deficits on tests of spatial memory in rats. *Eur. J. Neurosci.* **12**, 1714–1726
56. Fanardjian, V.V., Papoyan, E.V., Hovhannisyan, E.A., Melik-Moussian, A.B., Gevorkyan, O.V., and Pogossian, V.I. (2000) The role of some brain structures in the switching of the descending influences in operantly conditioned rats. *Neuroscience* **98**, 385–395

57. Burman, K., Darian-Smith, C., and Darian-Smith, I. (2000) Macaque red nucleus: origins of spinal and olivary projections and terminations of cortical inputs. *J. Comp. Neurol.* **423**, 179–196
58. Ito-Ishida, A., Miura, E., Emi, K., Matsuda, K., Iijima, T., Kondo, T., Kohda, K., Watanabe, M., and Yuzaki, M. (2008) Cbln1 regulates rapid formation and maintenance of excitatory synapses in mature cerebellar Purkinje cells *in vitro* and *in vivo*. *J. Neurosci.* **28**, 5920–5930
59. Iijima, T., Emi, K., and Yuzaki, M. (2009) Activity-dependent repression of Cbln1 expression: mechanism for developmental and homeostatic regulation of synapses in the cerebellum. *J. Neurosci.* **29**, 5425–5434
60. Barber, R.E. and Kwan, A.P. (1996) Partial characterization of the C-terminal non-collagenous domain (NC1) of collagen type X. *Biochem. J.* **320**, 479–485